

## A comparison of imaging sequences for sodium MR imaging on a 9.4T whole body machine

S. Romanzetti<sup>1</sup>, C. C. Mirkes<sup>1</sup>, D. Fiege<sup>1</sup>, A. A. Celik<sup>1</sup>, J. Felder<sup>1</sup>, and N. J. Shah<sup>1,2</sup>

<sup>1</sup>Institute of Neuroscience and Medicine, Research Centre Juelich, 52425 Juelich, NRW, Germany, <sup>2</sup>Department of Neurology, Faculty of Medicine, JARA, RWTH Aachen University, 52074 Aachen, Germany

### Introduction

MR Imaging of sodium, and generally of X-nuclei, given their low concentration in tissues and their fast relaxation properties will greatly benefit from the increase of signal at Ultra High Fields ( $\geq 7T$ ). Imaging of these nuclei typically requires the use of dedicated sequences and a high degree of optimisation. Several different approaches have been used in the past [1-7] with characteristic advantages and disadvantages. In this initial study, six sequences used for sodium imaging were compared on a 9.4T whole-body machine.

### Methods

Six sequences for <sup>23</sup>Na imaging were implemented on a Siemens (Erlangen, Germany) 9.4T whole-body scanner. The sequences were: Gradient Echo (GRE), 3D Cones (3DC), Twisted Projection Imaging (TPI), SPRITE, Cylindrical stack of radial spokes (CSRS), and 3D spokes (3DS). A novel, home-built RF coil comprising a birdcage transmitter and an 8-channel phased-array receiver was used during this study. A phantom with 6 compartments filled with gels at three sodium concentrations (30, 100, 150 mmol/l) and two agarose concentrations (2%, 6% w/w) was used in order to mimic the conditions found in the human brain. An automatic shimming procedure which made use of the sodium signal corrected the static field. The same set of shim values were used for all measurements. Sequence parameters are summarised in Table 1. In order to enable a fair compare, the sequences parameters were optimised such that the acquisition was under 10 minutes and at 95% of the imposed (first level) SAR limits.

### Results

Figure 1 shows the images acquired with the different methods. All images have sufficient SNR in order to distinguish the compartments with the lowest sodium concentration. Different levels of T2\* weighting are also visible. SNR values calculated for the compartment (outlined in yellow) of the lowest [<sup>23</sup>Na] (30 mmol/l) and highest [Agarose] (6% w/w) are summarised in Table 1.

### Discussion

Each sequence showed advantages and disadvantages that can be summarised as following: 3D GRE was the easiest sequence to implement. It shows good SNR, good image quality (PSF) but it suffers strongly from T2\* weighting due to rather long minimum achievable TE (> 1 ms). 3D

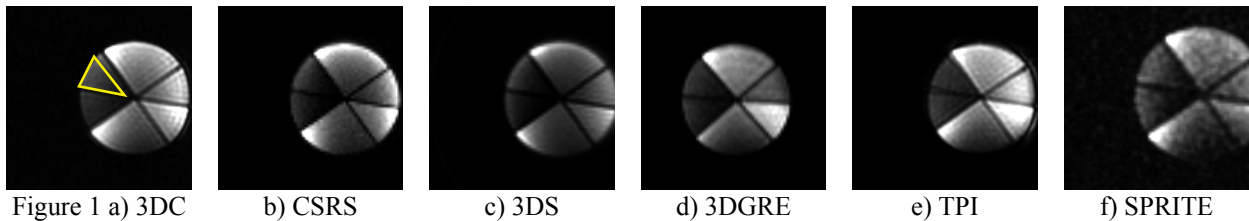


Figure 1 a) 3DC b) CSRS c) 3DS d) 3D GRE e) TPI f) SPRITE

Table 1

sequence	TR [ms]	TE [ms]	FA [°]	BW [Hz/px]	resolution	SNR
3DC	10	0.5	31	391	5x5x5	5.8
TPI	70	0.5	40	195	5x5x5	5.2
3D GRE	50	1.6	50	300	5x5x5	3.3
CSRS	50	0.8	50	320	5x5x5	2.3
3DS	50	0.4	50	320	5x5x5	2.2
SPRITE	1.0	0.3	2	3125	6x6x6	2.7

cones and TPI seem to deliver the highest SNR as a result of their rather uniform k-space sampling and their ultrashort TE, which effectively limits T2\* weighting. However, they seem to be prone to off-resonance effects, more prominent for TPI, which leads to the use of very high bandwidths. The CSRS and 3DS show limited T2\* weighting, comparable to TPI and 3DC, but the less uniform k-space sampling influences the SNR performance of these sequences. CSRS requires less radial spokes than 3DS but has longer TE due to phase encoder, especially for large k-space matrices. SPRITE shows no T2\* weighting, but images show the lowest SNR due to the low flip angle used (about 2°), as imposed by the SAR constraints.

### Conclusions

The initial results of this study seems to indicate that non-radial sequences, and in particular 3D Cones, are better suited to match the general requirements of high SNR and short echo times which are needed for sodium imaging at high fields.

### References

(1) Boada, et al. MRM 37: 706-15; (2) Gurney, PT et al., MRM 55: 575-82; (3) Nilles-Vallespin et al., MRM 57:74-81; (4) R. Stobbe et al., Ann Neurol; 66:55-62, (5) S. Romanzetti et al. Proc. ISMRM (2008), (6) R. Parish et al.,MRM 38: 653-61; (7) Robson MD et al., J Comp Assist Tomogr 27: 824-26